



Heterogeneous circulating tumor cells correlate with responses to neoadjuvant chemotherapy and prognosis in patients with locally advanced breast cancer

Ge Ma^{1,2} · Jingyi Wang³ · Jingyue Fu¹ · Rui Chen¹ · Mengdi Liang¹ · Minghui Li¹ · Tiansong Xia^{1,2} · Xiaoan Liu¹ · Shui Wang^{1,2} 

Received: 5 August 2022 / Accepted: 5 April 2023

© The Author(s), under exclusive licence to Springer Science+Business Media, LLC, part of Springer Nature 2023

Abstract

Neoadjuvant chemotherapy (NCT) is the standard treatment for patients with locally advanced breast cancer (LABC). The predictive value of heterogeneous circulating tumor cells (CTCs) in NCT response has not been determined. All patients were staged as LABC, and blood samples were collected at the time of biopsy, and after the first and eighth NCT courses. Patients were divided into High responders (High-R) and Low responders (Low-R) according to Miller–Payne system and changes in Ki-67 levels after NCT treatment. A novel SE-i-FISH strategy was applied to detect CTCs. Heterogeneities were successfully analyzed in patients undergoing NCT. Total CTCs increased continuously and were higher in Low-R group, while in High-R group, CTCs increased slightly during NCT before returning to baseline levels. Triploid and tetraploid chromosome 8 increased in Low-R but not High-R group. The number of small CTCs in Low-R group increased significantly until the last sample, however, remained constant in High-R group. The patients with more CTCs had shorter PFS and OS than those with less CTCs after the eighth course of NCT. Total CTCs following NCT could predict patients' responses. More detailed characterizations of CTC blood profiles may improve predictive capacity and treatments of LABC.

Keywords Neoplastic cells, circulating · Breast neoplasms · Neoadjuvant therapy · Biomarkers

Ge Ma, Jingyi Wang and Jingyue Fu contributed equally to this work.

✉ Tiansong Xia
xiatsswms@163.com

✉ Xiaoan Liu
liuxiaoan@126.com

✉ Shui Wang
shwang@njmu.edu.cn

¹ Department of Breast Surgery, The First Affiliated Hospital With Nanjing Medical University, 300 Guang-Zhou Road, Nanjing 210029, China

² Jiangsu Key Lab of Cancer Biomarkers, Prevention and Treatment, Jiangsu Collaborative Innovation Center for Cancer Personalized Medicine, School of Public Health, Nanjing Medical University, Nanjing 211166, China

³ Department of Breast Surgery, The Affiliated Changzhou No. 2 People's Hospital of Nanjing Medical University, 29 Xinglong Lane, Changzhou 213003, China

Introduction

Breast cancer is the most common malignant tumor in women, and neoadjuvant chemotherapy (NCT) is the standard of care for patients with locally advanced breast cancer (LABC) [1]. However, a large number of patients with breast cancer respond poorly to standard treatment, and only a small number of patients achieve a complete or optimal response. In addition, chemotherapy can induce a significant, unexpected “opposite effect” that accelerates critical metastatic steps in malignancy, rather than inhibiting them [2]. Tumor heterogeneity may account for different therapeutic effects and should be appropriately addressed in treatment response evaluation. NCT should achieve two main objectives: shrinkage of the primary tumor and eradication of blood-borne tumor cell dissemination [3]. However, in practice due to the lack of standard testing criteria, the second objective is almost entirely overlooked by current NCT assessments despite metastasis being the primary cause of death in breast cancer patients [4].

Circulating tumor cells (CTCs) are released from the primary tumor into the blood stream and are considered to be the initiators of metastasis at distant organ sites [5]. In early breast cancer, CTC detection rates are 8–56%, according to different methods [6–8]. Numerous studies have demonstrated that the presence of CTCs in breast cancer is a marker of poor prognosis [9, 10]. In the case of LABC, the German Breast Group demonstrated that detection of CTCs prior to NCT is an independent prognostic factor of impaired clinical outcome and is particularly effective when combined with pCR [11]. Although sufficient evidence exists to recognize the prognostic value of CTCs as an example of high-quality evidence-based medicine, complete elucidation of the quantitative changes and molecular characterization of CTCs during NCT have not been carried out, which may serve to improve the unfavorable prognoses of patients.

CTCs are present at very low concentrations in peripheral blood, and therefore, highly sensitive assays are required. Conventional detection strategies include two steps, enrichment and detection (or characterization). The Cell Search System is unable to effectively detect multi-functional mesenchymal CTCs while real-time PCR (RT-PCR)-based tumor cell detection methods cannot accurately measure CTC numbers by gene expression measurement [12]. Recently, a novel CTC detection strategy, subtraction enrichment, and immunostaining fluorescence in situ hybridization (SE-i-FISH) have been applied. This technique integrates both steps and achieves much higher sensitivity; negative selection, which does not limit CTC isolation to those expressing particular tumor markers, is used to enrich CTCs using the leukocyte marker CD45 [13]. This system is an innovative means to detect chromosome aneuploidy with synchronous detection of the tumor biomarkers listed above. Aneuploidy may result in genomic instability [14]. In fact, several studies have described it as the most common feature of malignant tumor cells [15, 16]. Further, using SE-i-FISH enables observation of CTC morphological features. For instance, small CTCs (<5 μm) as well as circulating tumor microemboli (CTM; a cluster of two or more CTCs) can be distinguished from CTCs in the traditional sense. In summary, benefits of SE-i-FISH include not only improved enumeration of CTCs, but also more detailed characterization and analytical opportunities that may be investigated during NCT assessments.

The aim of this study was to evaluate the predictive power of heterogeneous CTCs with respect to LABC patients receiving NCT. Further, we explore the future prospects for liquid biopsy and characterization of heterogeneous CTCs in NCT.

Materials and methods

Patients and sample collection

Written informed consent was obtained from all patients prior to enrollment in the study. All procedures were approved by Institutional Review Boards of the First Affiliated Hospital with Nanjing Medical University.

A total of 45 patients diagnosed with LABC were enrolled at the First Affiliated Hospital of Nanjing Medical University from October 2016 to November 2017. Breast cancer in all patients was confirmed by core biopsy. The pathological report, including histological type, hormone receptors, HER-2 status, and Ki-67 index were provided by the Pathology Department of the First Affiliated Hospital of Nanjing Medical University. All patients were staged as LABC and received an EC \times 4–T \times 4 NCT regimen (epirubicin 90 mg/m² iv d1, cyclophosphamide 600 mg/m² iv d1 on a 21 days cycle for four cycles, then docetaxel 80 mg/m² iv d1, on a 21 days cycle for four cycles). Blood samples (6 ml) were collected for CTC detection pre-treatment (at time of biopsy) and after the first and eighth courses of chemotherapy. Complete blood counts (lymphocyte, neutrophils, and platelets) referred to the blood cell analysis reported by the Clinical Laboratory of the First Affiliated Hospital of Nanjing Medical University. All patients with LABC underwent surgery. The Ki-67 values from the postoperative and preoperative biopsy pathology reports were compared and used to evaluate the NCT response. All patients were assigned to one of two groups, those in the Low-Responder (Low-R) group had a higher Ki-67 index following NCT, compared to the 66.67% basal Ki-67 value prior to NCT; alternatively, the High-Responder (High-R) group had a lower Ki-67 index. In addition, the Miller–Payne system was applied for NCT response classification [17].

Immunofluorescence staining and SE-i-FISH

In this study, we applied the subtraction enrichment (SE) and immunostaining-FISH (i-FISH®) platform for CTC detection and characterization, which has been reported previous [18–20]. Experiments were performed according to the operation manual (Cytelligen, San Diego, CA, USA). Briefly, peripheral blood was collected into Cytelligen tubes containing ACD anti-coagulant (Becton Dickinson, Franklin Lakes, NJ, USA) and centrifuged at 450 \times g for 5 min. All sedimented cells were subsequently loaded onto the top of 3 ml non-hematopoietic cell separation matrix for immediate processing by density gradient centrifugation.

Supernatants above the red blood cell layer were collected and incubated with a cocktail including

anti-leukocyte antibody (CD45) immunomagnetic beads at 23–25 °C for 15 min with gentle shaking. Subsequently, the solution was subjected to magnetic separation. The bead-free solution was spun at 500 × g for 2 min. Sedimented cells were thoroughly mixed with cell fixative and applied to coated CTC slides for subsequent i-FISH analysis.

Air-dried samples on coated CTC slides were hybridized with centromere probe 8 (CEP8) (Abbott Laboratories, Abbott Park, IL, USA) for 3 h, followed by antibody staining by incubation with Alexa Fluor (AF) 594-anti-CD45(clone: 9.4), Cy5-anti-EpCAM (epithelial cell adhesion marker) (clone: 9C4), Cy7-anti-vimentin (clone: 1D3), and AF488-anti-CD31 (Cytelligen, San Diego, CA, USA) (clone: WM59) at room temperature for 30 min.

Metafer-i-FISH® automated CTC 3D scanning and image analysis

Image capture, as well as CTC identification and analysis were performed using the automated Metafer-i-FISH®-CTC 3D scanning and analyzing system (Carl Zeiss, Oberkochen, Germany; MetaSystems, Altlussheim, Germany; and Cytelligen, San Diego, CA, USA). Briefly, CTC slides loaded onto a fluorescence microscope (AXIO Imager Z2) stage were subjected to automated full X–Y plane scanning with cross Z-sectioning of all cells performed at a 1 mm step depth, with fluorescence signal acquisition of all color channels. Automated image processing, classification, and statistical analysis were performed to comprehensively evaluate cell size, cell cluster, tumor biomarker expression, and chromosome ploidy. A cell was judged to be CTC if it matched either of the following criteria:

- (1) DAPI⁺CD45⁻CD31⁻EpCAM[±]vimentin[±]chromosome 8 (Chr8) aneuploidy or polyploidy
- (2) DAPI⁺CD45⁻CD31⁻chr8 diploidy/ EpCAM[±] or/and vimentin[±]

Statistical analysis

Results are expressed as the mean ± SD. The number of CTCs and different heterogeneities were analyzed by repetitive measurement deviation analysis between the High-R and Low-R groups. Multiple comparison analysis corrected by Tukey's test was used to analyze the differences within groups. Chi-square analysis and multivariate analysis were used to determine the chemotherapy responses in patients with different clinicopathological features. To evaluate the predictive value of CTC occurrence in distinguishing chemotherapy-resistant patients from sensitive ones, we plotted receiver operating characteristic (ROC) curves and calculated the area under the curves (AUCs). The ROC curves

of total and heterogeneous CTC numbers were generated at three time points. The Δ value, defined as the difference between the two measurements, was also analyzed by ROC curve. Correlation coefficients of two variables were calculated with Pearson analysis. Survival analysis was performed using Log-rank test. All statistical analyses were performed with SPSS version 21.0 (SPSS, IBM; Chicago, IL, USA), and all *p* values were two-tailed with 5% significance levels.

Results

Establishment of SE-i-FISH for breast cancer CTCs in situ phenotype and karyotype identification

SE-i-FISH was optimized to monitor breast cancer CTCs expressing tumor biomarkers and Chr8 aneuploidy. Immunofluorescence staining of CTCs with anti-EpCAM and mesenchymal marker vimentin showed distinct intracellular staining for both EpCAM and vimentin. (Fig. 1).

Analysis of CTCs detected by patient classification

The CTC-positive detection rate was 43/45 in LABC patients (95.6%) before NCT, and 100% following the first course of NCT and post-NCT.

Patients were divided into two groups according to changes in Ki-67. The High-R group was composed of 22 patients (48.9%) and the Low-R group of 23 patients (51.1%). According to the Miller–Payne system, 8/45 patients obtained >90% loss of tumor cells (grade 4–5), while the other 37 patients were assigned to grade 1–3. All eight grade 4–5 patients belonged to the High-R group when sorted according to Ki-67 changes.

Chemotherapy responses were not associated with any of the patients' clinical and pathologic characteristics (Table 1, Chi-square test was used to analyze the influence of different factors on chemotherapy response). Patient clinicopathological features and their association with CTC detection are also shown in Table 1. The CTC-positive rate was not correlated with age, HER-2 status, or lymph node metastasis. However, patients with more than two lymph node metastases exhibited significantly higher numbers of CTCs (repetitive measurement deviation analysis, *p* = 0.029). Further, during NCT, CTC numbers increased in patients with more than two metastatic lymph nodes (*p* < 0.001 and 0.043 for post-1st NCT and post-NCT, respectively, additional file 1, Fig. S1A). Specifically, the number of CTC was high only during NCT in High-R group yet was continuously elevated in the Low-R group. Alternatively, for patients with two or less metastatic lymph nodes, the CTC number showed a downward trend following the initial rise in the High-R

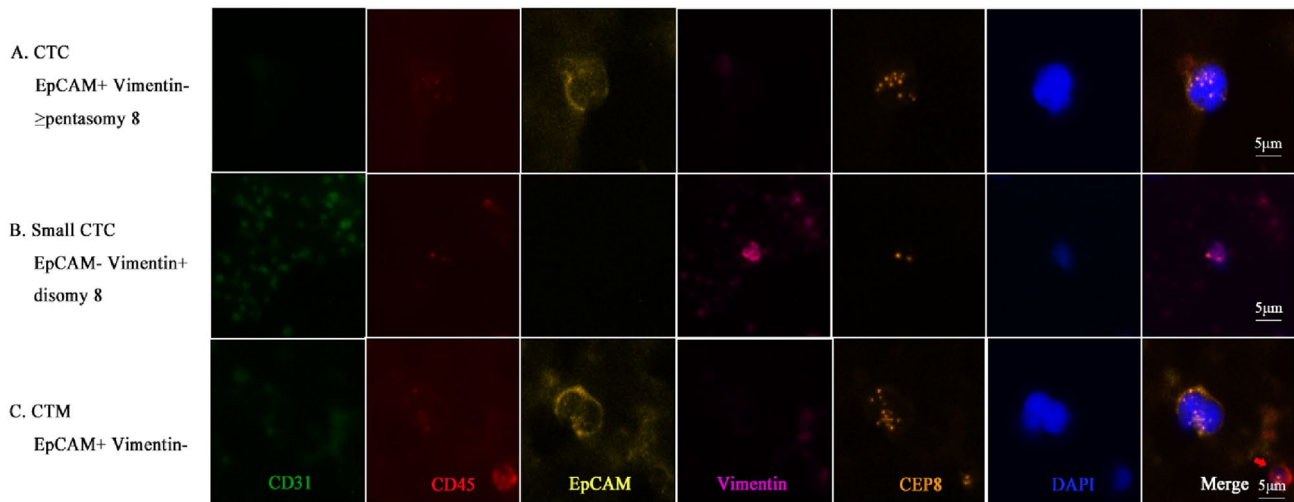


Fig. 1 Detection of CTCs by SE-iFISH. **A** A CTC with EpCAM⁺ vimentin⁻ ≥pentasomy 8. **B** A small CTC with EpCAM⁻ vimentin⁺ disomy 8. **C** A CTM with EpCAM⁺ vimentin⁻ by SE-iFISH. (WBC: red arrow)

group; while in the Low-R group, the number was found to steadily increase (Additional file 1, Fig. S1A and B).

CTC numbers analyzed by patient group: correlation with NCT effect

A typical fluorescent photograph of a CTC is shown in Fig. 2A. In general, the number of CTCs increased after the first NCT cycle compared to pre-NCT levels ($p < 0.001$). This trend continued post-NCT ($p = 0.001$, Fig. 2B). The number of CTCs was higher in the Low-R group (repetitive measurement deviation analysis, $p = 0.042$). There were no significant differences in CTC number between High-R and Low-R groups before NCT or after the first course of NCT (Fig. 2C). However, following the eighth NCT course, the difference between the two groups was significant ($p = 0.028$). The CTC number increased slightly ($p = 0.051$), then decreased to baseline in the High-R group, while in the Low-R group, the number of CTCs continuously increased continuously during NCT (Fig. 2D).

According to the Miller–Payne system, the CTC number of grade 1–3 patients increased significantly and continuously following all NCT courses compared to grade 4–5 patients (Fig. 2E and F).

Chromosome 8 karyotype changes between patients with different NCT responses

The existence of heterogeneous polysomic Chr8 confirmed the marked heterogeneity of breast cancer CTCs (Fig. 3A); while the ratios of CTCs with different Chr8 ploidies changed during treatment (Fig. 3B). The frequencies of CTCs with triploid Chr8 copy numbers were 28, 34, and 45%

at the three successive time points, and the corresponding tetraploid Chr8 numbers were 14, 27, and 24%, respectively. Analysis of the occurrence of triploid, tetraploid, pentaploid, or higher Chr8 copies in CTCs according to NCT response showed that the number of CTCs containing Chr8 triploidy and tetraploidy was higher in the Low-R group than in the High-R group following NCT; however, this effect was not observed pre- or post-initial NCT ($p = 0.017$ and 0.009 for triploidy and tetraploidy, respectively, Fig. 3C and G). Compared to the CTC number before NCT, an increase in Chr8 triploidy and tetraploidy was observed in the Low-R group post-first NCT ($p = 0.003$ and 0.010 , respectively) and post-NCT ($p = 0.002$ both in triploid and tetraploid Chr8), while in the High-R group, Chr8 triploidy only increased post-first NCT, after which it returned to baseline. No increase in tetraploid Chr8 was observed in CTCs following NCT in High-R group (Fig. 3D and H).

When patients were classified by the Miller–Payne system, the trends observed in CTC Chr8 triploidy, tetraploidy, and multiploid variations were similar to the ki-67 group mode (Fig. 3 E, F, I, J).

Correlation of the number of small-size CTCs with NCT response

A vimentin⁺ small-size CTC is depicted in Fig. 4A (left). The number of small CTCs ($< 5 \mu\text{m}$) increased after the first NCT cycle ($p < 0.001$), after which it remained elevated post-NCT ($p = 0.001$), consistent with the overall changes observed in CTCs (Fig. 4B). Further, the number of small CTCs in Low-R patients was significantly higher during the final time point after the eighth course of NCT ($p = 0.038$; Fig. 4C). This difference, however, reflected growth in the

Table 1 CTC numbers of patients with different clinical characteristics

Factors	Total	High-R	Low-R	Statistical test	Multivariate analysis		Repetitive measurement deviation analysis					
					OR	<i>p</i> value	pre-NCT	post-1st NCT	post-NCT	<i>p</i> value ¹	<i>p</i> value ²	
Total	45	22	23									
Age				0.181		0.082						
<50	22	13	9		1		8.18 ± 7.82	111.18 ± 160.25	32.55 ± 45.48		<0.001	0.545
≥50	23	9	14		3.371 [0.855–13.284]	0.820	6.44 ± 5.53	49.78 ± 63.22	66.91 ± 93.04		0.001	0.111
Her-2 status				0.848								
Negative	28	14	14		1		6.72 ± 6.18	70.14 ± 130.58	40.28 ± 61.69			
Positive	17	8	9		1.192 [0.262–5.414]	0.359	8.31 ± 7.73	97.31 ± 110.92	67.94 ± 94.06		0.002	0.117
Molecular subtype				0.815								
Hormone + Her-2/+	33	17	16		1		7.30 ± 6.82	58.49 ± 76.48	47.12 ± 77.27			
TNBC	10	4	6		0.281 [0.012–6.865]		7.25 ± 6.74	138.42 ± 196.83	58.33 ± 70.71			
Hormone-Her-2 +	2	1	1		0.089 [0.02–4.059]		8.50 ± 3.54	140.00 ± 195.16	124.00 ± 4.24			
Lymph node				0.100		0.064						
≤2	23	14	9		1		6.63 ± 6.77	48.92 ± 52.36	34.83 ± 57.57			
>2	22	8	14		3.825 [0.923–15.859]		8.05 ± 6.76	115.81 ± 166.65	67.57 ± 89.14		<0.001	0.029

P value1: different timepoints. *P* value1 represents the within-Subject Factor. The time effect is a special independent variable, to see if the dependent variable changes over time

P value2: clinical characteristics. *P* value2 represents the between-group effect (group)

Statistical test: Chi-square test or Fisher's exact test

The parameters of bold showed a significant difference ($P < 0.05$)

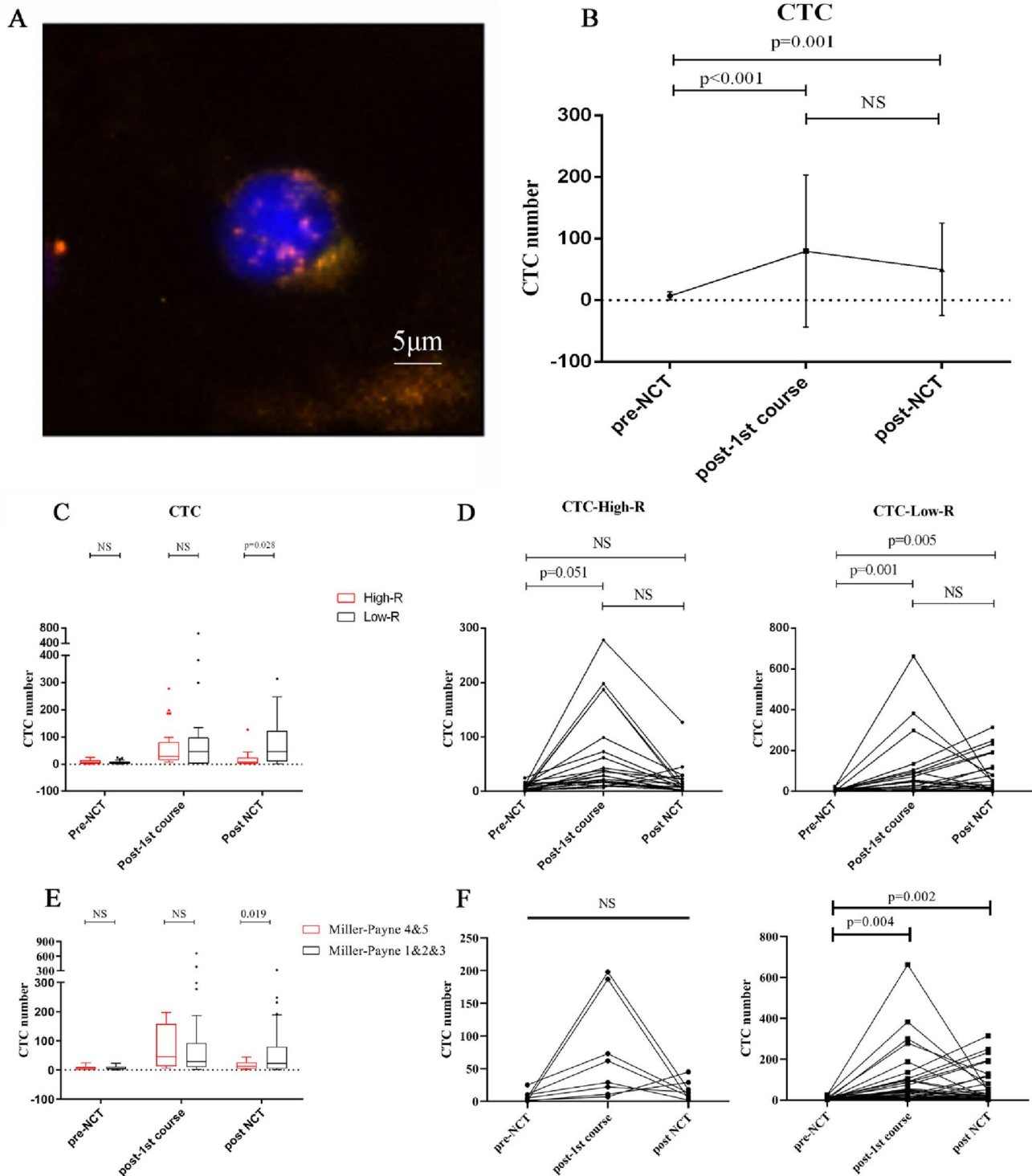


Fig. 2 CTC levels in patients during NCT. **A** A typical fluorescent photograph of a CTC. **B** Trend in total CTCs during treatment. Measurements after the eighth course of treatment revealed more CTCs in patients receiving NCT. **C** The difference in CTC numbers between the two response groups at three time points (Ki-67 index mode). There was no significant difference in number of CTCs until the first course of NCT. Low-R patients had higher levels of CTC than High-R patients before surgery. **D** The CTC number increased slightly ($p=0.051$) but then returned to baseline in the High-R group;

in contrast, the number increased continuously during NCT in the Low-R group (Ki-67 index mode). **E** The difference in CTC numbers between Miller–Payne grades 1–3, and 4–5 at three time points. There was no significant difference in CTC number until the first course NCT. Miller–Payne grade 1–3 patients had higher levels of CTCs than Miller–Payne grade 4–5 patients before surgery. **F** No significant changes in CTC number were detected in the Miller–Payne 4–5 group during NCT; in contrast, the CTC number increased continuously during NCT in the grade 1–3 group

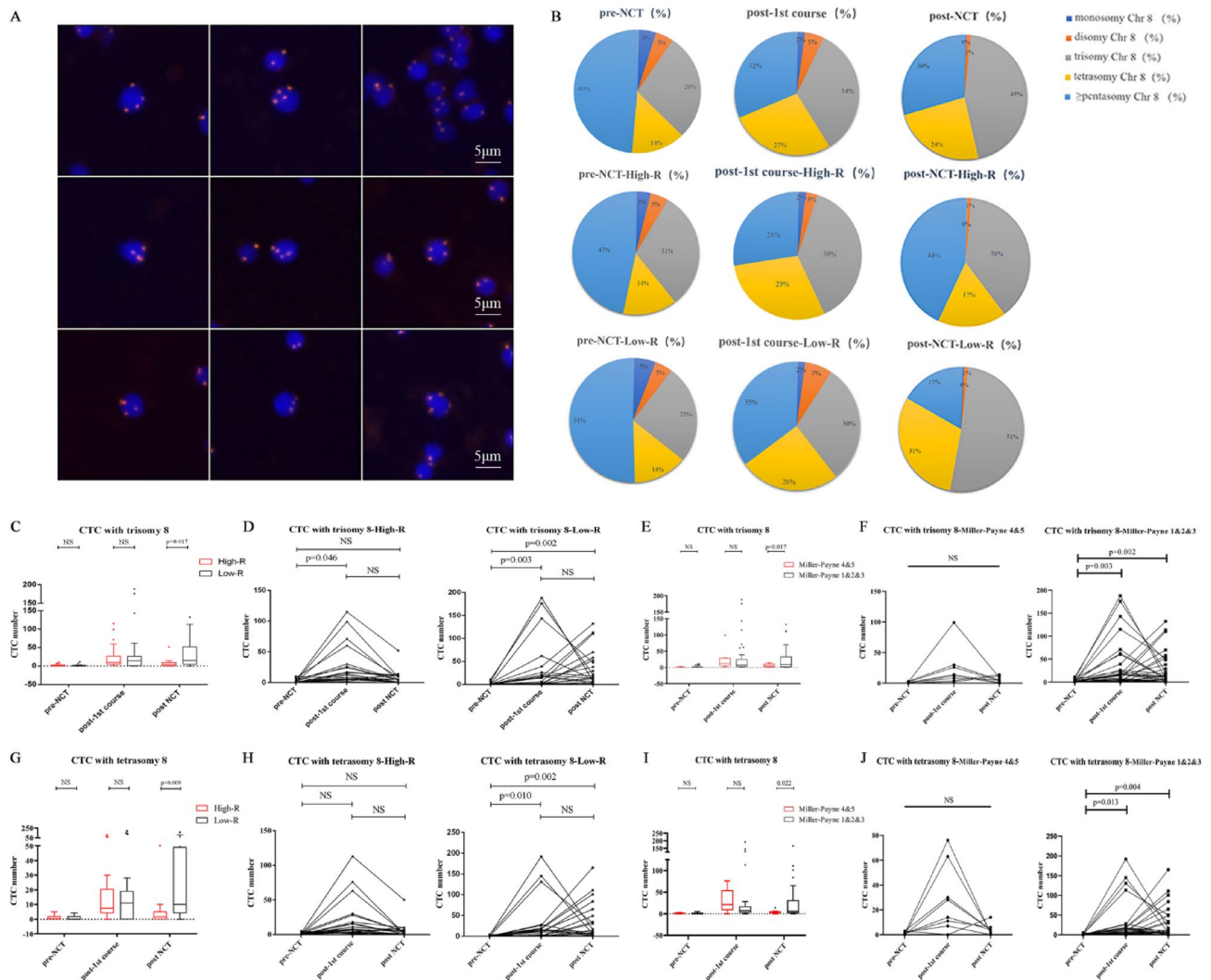


Fig. 3 Changes in CTC numbers and proportion with different chromosome 8 karyotypes between patients with different responses to NCT. **A** Images of CTCs with different chromosome 8 ploidy. CTC nuclei were stained with DAPI (blue) and chromosome 8 were imaged with centromere probe 8 spectrum orange (red dots). **B** Quantitative composition of heterogeneous CTCs with different chromosome 8 ploidy in entire populations of CTCs detected in High-R and Low-R groups at three time points. **C** Comparison of trisomy 8 CTCs between the two response groups (Ki-67 index mode). No significant differences were observed between High-R and Low-R patients at the first two time points. The trisomy 8 CTC number increased in the Low-R group after the eighth course. **D** Comparison of trisomy 8 heterogeneous CTCs over the course of NCT (Ki-67 index mode). Compared to the CTC number before NCT, the triploid chromosome 8 CTCs increased in the Low-R group post-first NCT and post-NCT. Triploid chromosome 8 increased post-first NCT and returned to baseline level in the High-R group post-eighth NCT. **E** Comparison of trisomy 8 CTCs between the two response groups. No significant differences were observed between Miller-Payne grade 4–5 and 1–3 patients at the first two time points. The trisomy 8 CTC num-

ber increased in the Miller-Payne grade 1–3 group after the eighth course. **F** Compared to the CTC number before NCT, triploid chromosome 8 CTCs increased in Miller-Payne grade 1–3 patients post-first NCT and post-NCT. **G** Comparison of tetrasomy 8 CTCs between the two response groups (Ki-67 index mode). The tetrasomy 8 CTC number was higher in the Low-R group than the High-R group after the eighth course. There was no difference between these two groups previously. **H** Comparison of tetrasomy 8 heterogeneous CTCs over the course of NCT (Ki-67 index mode). No increase of tetraploid chromosome 8 was observed in CTCs over the course of NCT in High-R patients. The number of CTCs with tetrasomy 8 increased significantly until the last detection in Low-R patients. **I** Comparison of tetrasomy 8 CTCs between the two groups. The tetrasomy 8 CTC number was higher in the Miller-Payne grade 1–3 group than the Miller-Payne grade 4–5 group after the eighth NCT course. There was no difference between these two groups previously. **J** No increase in tetraploid chromosome 8 was observed in CTCs over the course of NCT in Miller-Payne grade 4–5 patients. The number of CTCs with tetrasomy 8 increased significantly until the last detection in the Miller-Payne grade 1–3 group

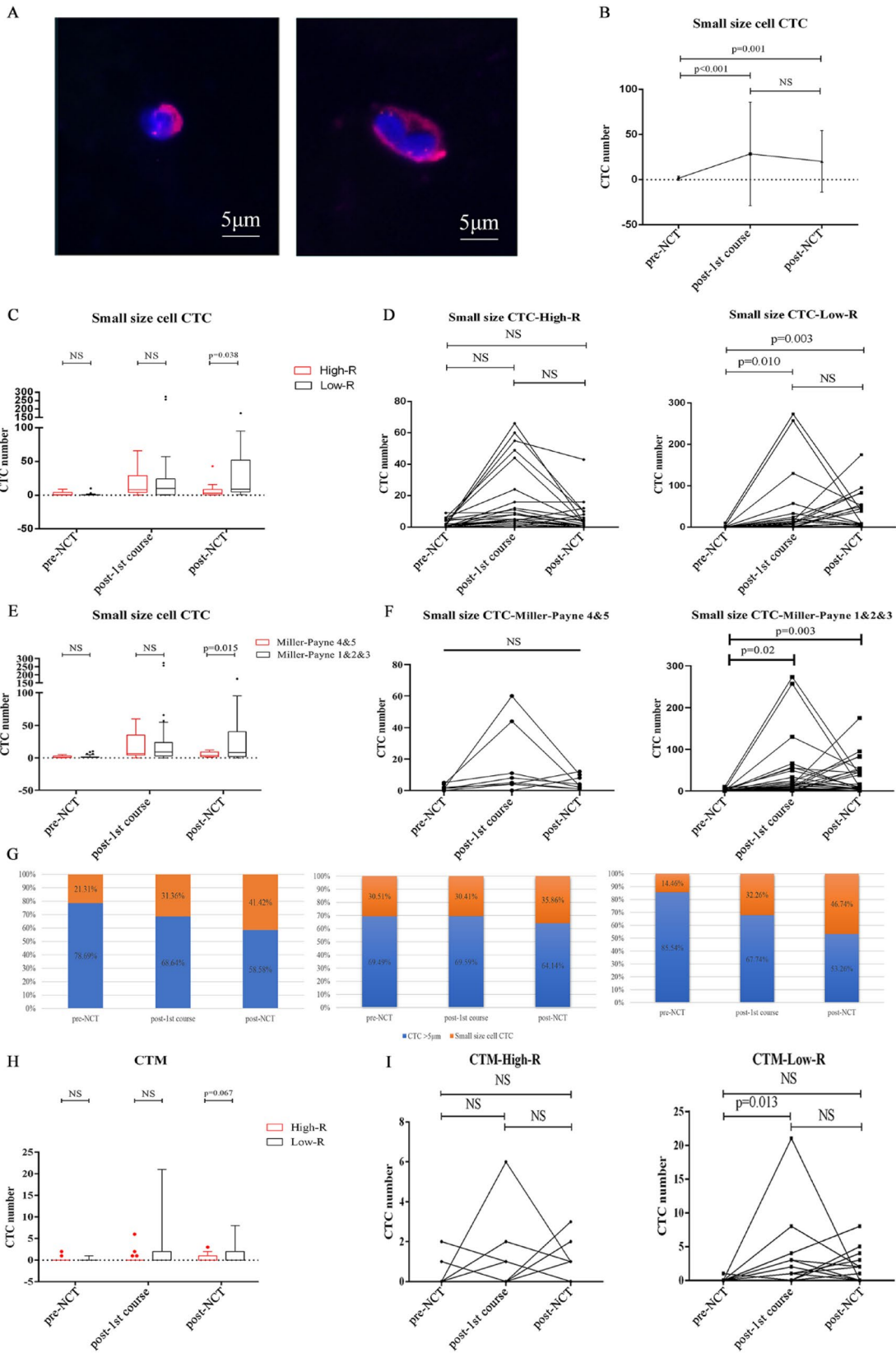


Fig. 4 Correlation of small-size CTCs, CTM, and chemotherapeutic effect. **A** Left, photograph of a small-size CTC; Right, image of a two CTC cluster microembolus. **B** Quantitative comparison of small CTCs. The number of small-size CTCs continued to increase during NCT. **C** Compared to the High-R group (Ki-67 index mode), the number of small CTCs in the Low-R group increased significantly after the eighth course of NCT. **D** The number of small CTCs in Low-R patients rose after the first course of NCT and then remained constant at a comparatively high level. The CTC level of High-R patients remained approximately constant during NCT (Ki-67 index mode). **E** Compared to the Miller–Payne grade 4–5 group, the number of small CTCs in the Miller–Payne grade 1–3 group increased significantly after the eighth course of NCT. **F** The number of small CTCs in Miller–Payne grade 1–3 patients rose after the first course of NCT, then remained constant at a comparatively high level. **G** Overall proportion changes and changes within response groups. The proportion of small CTCs increased during NCT. The proportion of small CTC in High-R patients rose from 30.5% to 35.9%, the change in the Low-R was from 14.5 to 46.7%. **H** No significant change in CTM numbers was found for the different patient groups following NCT. **I** Post-first course samples showed significantly higher CTM numbers in Low-R patients compared to pre-NCT samples. CTM numbers in the High-R group remained approximately constant during NCT

number of small CTCs after the first course ($p=0.010$), which then plateaued at a comparatively high level ($p=0.003$). Unlike the Low-R group, the CTC level of the High-R group remained approximately constant throughout the NCT process (Fig. 4D). The percentage of small CTCs in the High-R group were 30.5%, 30.4%, and 35.9%, respectively, at the three timepoints (Fig. 4G). The corresponding data for the Low-R group were 14.5%, 32.3%, and 46.7%. Additionally, the patients designated as Miller–Payne grade 1–3 exhibited the same trend in variation as that observed in the Low-R group, while grade 4–5 was observed to be the same as the High-R group (Fig. 4E, F).

CTM of LABC patients during NCT

A vimentin⁺ CTM is depicted in Fig. 4A (right). No significant changes were observed in CTM numbers following the eighth course of NCT (repetitive measurement deviation analysis). However, the results in Low-R patients following the first course of treatment showed apparently higher numbers of CTM compared to those before NCT (Fig. 4I). No significant differences were observed between High-R and Low-R groups at the other timepoints; the CTM increase in the Low-R group only slightly exceeded the significance level ($p \leq 0.05$) at the second time point, post-first course ($p=0.067$) (Fig. 4H).

CTC, mesenchymal phenotypes, and NCT sensitivity

Next, CTCs were grouped according to the presence or absence of the mesenchymal marker vimentin (Fig. 5A). The number of total and small vimentin⁻ CTCs increased during NCT. Further, the vimentin⁺ CTCs increased after the first

NCT course, and decreased after the last course, whereas small vimentin⁺ CTCs increased after the first course, then remained approximately constant. Patients in the Low-R group displayed higher numbers of vimentin⁻ CTCs and small CTCs after NCT ($p=0.060$ and 0.038 for CTCs and small CTCs, respectively, Fig. 5G and I). Conversely, no difference was found in vimentin⁺ CTCs, while an increased number of vimentin⁺ small CTCs was detected in the High-R group following the first course of NCT (Fig. 5C and E). Further, vimentin⁻ CTCs remained constant over the course of NCT treatment in the High-R group and increased in the Low-R group at which level it remained relatively constant until surgery ($p=0.002$ and 0.008 for the first and eighth courses of NCT, respectively, Fig. 5H). In contrast, vimentin⁺ CTCs showed no significant changes during NCT (Fig. 5D). In terms of vimentin⁺ small CTCs, no significant changes in number were detected in the Low-R group during NCT. In contrast, vimentin⁺ small CTCs increased post-first NCT course after which they returned to baseline in the High-R group (Fig. 5F). Vimentin⁻ small CTCs showed no significant change in the High-R group, but in the Low-R group an obvious increase was observed after the first course of NCT, then levels remained high (Fig. 5J).

Cumulatively, these data indicate a possible correlation between low response to NCT and increased vimentin⁻ CTCs with no reduction in vimentin⁺ CTC numbers. The proportion of total vimentin⁻ CTCs confirmed this conclusion. In the Low-R group, the percentage of vimentin⁻ small CTCs rose from 10% before NCT to 46% after completion (Fig. 5B).

Correlation between CTCs and non-cancer cells (lymphocyte, neutrophils, and platelets), CTCs and cancer biomarkers during NCT

The relationships between aneuploid CTCs and non-cancer cells (lymphocyte, neutrophils and platelets) were shown in Fig. S2 (Additional file 2). The number of CTCs was positively correlated with neutrophils ($p=0.005$, $r=0.416$) and platelets ($p=0.421$, $r=0.004$) before treatment, however, these correlations were not apparent following the first course of NCT. Moreover, no correlation was observed between CTCs and the lymphocyte, tumor markers CEA, CA12-5, and CA15-3 (Additional files 2 and 3, Figs. S2 and S3).

Predictive value of CTC numbers

ROC curve analyses indicated that the CTC total, as well as the individual heterogeneities, effectively predicted the NCT response after the eighth course of NCT. The AUCs for heterogeneous CTCs after the eighth course of NCT were 0.770 (95% confidence interval (CI) 0.630–0.909), 0.776

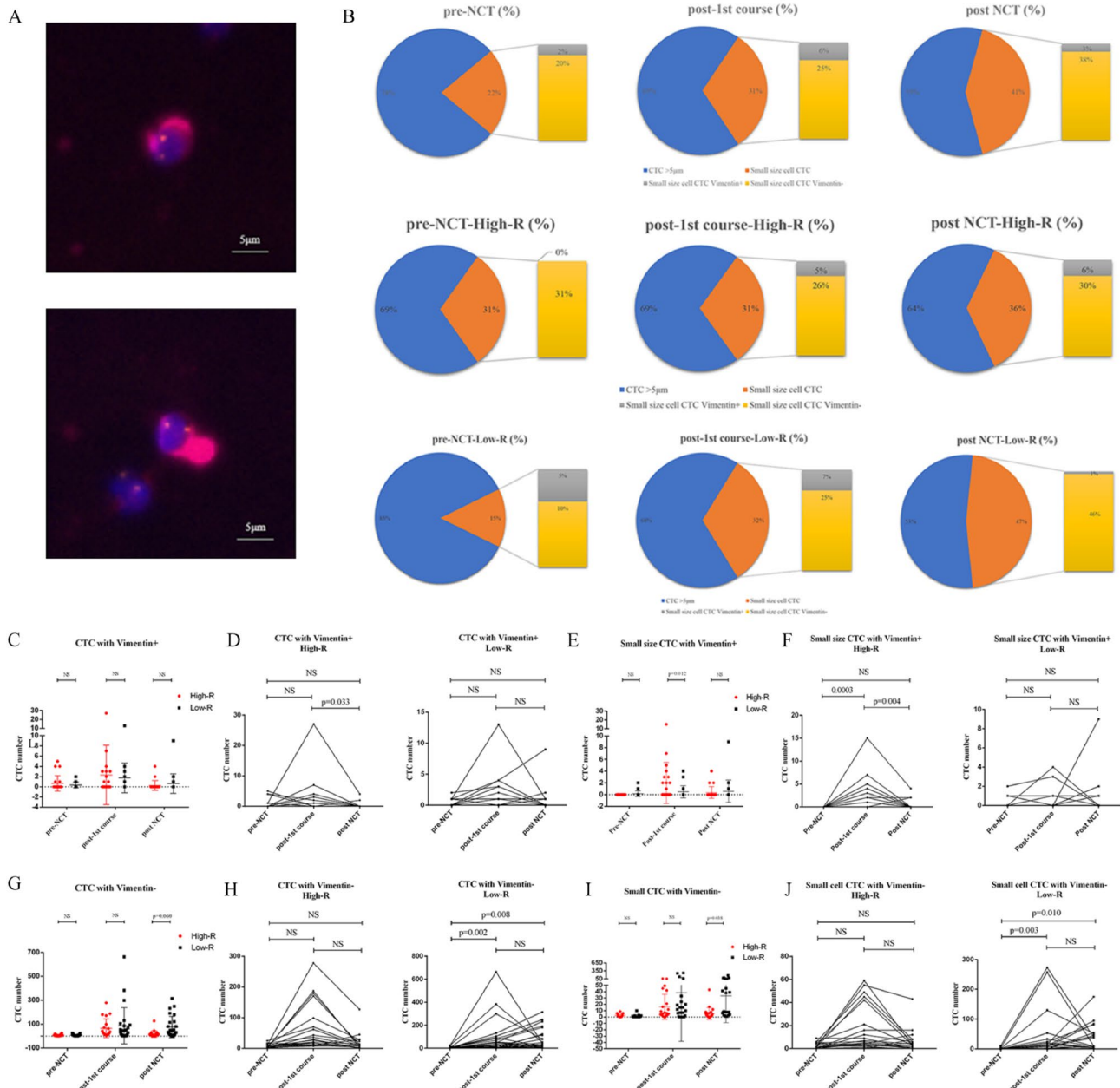


Fig. 5 CTCs with different mesenchymal phenotype exhibited different sensitivities to NCT. **A** Images of CTCs and small-size cell CTCs with vimentin+. Number of total CTCs and small CTCs with vimentin- increased during NCT. Total vimentin+CTCs increased after the first course and decreased after the last course. Small vimentin+CTCs increased after the -first course and then remained constant. **C** and **E** No differences were found in vimentin+total CTC occurrence between the two response groups. However, more vimentin+small CTCs were detected in the High-R group after the first course of NCT. **D** The number of total vimentin+CTCs did not change during NCT. **F** The vimentin+CTC number increased post-first NCT and returned to baseline level in the High-R group. No sig-

nificant changes in number were detected in the Low-R group during NCT. **G** and **I** Patients in the Low-R group displayed higher numbers of vimentin CTCs and small CTCs after NCT than the High-R group. **H** Vimentin- CTCs remained constant in the High-R group, but in the Low-R group, increased after the first course of NCT and remained at the same high level until surgery. **J** Small vimentin- CTCs showed no change in the High-R group but increased after the first course of NCT and remained at the same high level in Low-R group. **B** The proportion of small CTCs with different mesenchymal phenotypes. In the Low-R group, the percentage of vimentin- small CTCs rose from 10% before NCT to 47% after all courses

(95% CI 0.642–0.910), 0.777 (95% CI 0.640–0.913), 0.784 (95% CI 0.649–0.918), 0.772 (95% CI 0.632–0.911) and 0.792 (95% CI 0.663–0.922) for overall CTCs, small CTCs, trisomy 8 CTCs, tetrasomy 8 CTCs, vimentin⁻ CTCs, and vimentin⁻ small CTCs, respectively (all *p* values < 0.05, Fig. 6A). Similarly, the Δ value2 (difference between the third and the first measurements) was an effective predictor of outcome. The AUCs for this measurement were 0.797 (95% CI 0.670–0.925), 0.822 (95% CI 0.702–0.942), 0.776 (95% CI 0.641–0.910), 0.804 (95% CI 0.676–0.933), 0.794 (95% CI 0.666–0.923), and 0.845 (95% CI 0.732–0.958), respectively (all *p* values < 0.05, Fig. 6B). Considering the samples after only the first course of treatment, only the Δ value1 (difference between the second and the first measurements) of small vimentin⁻ CTCs exhibited significant diagnostic value (AUC 0.566; 95% CI 0.396–0.737; Fig. 6C). However, a lower degree of diagnostic efficiency was achieved when the Miller–Payne system was adopted,

which may be related to the unbalanced sample size (Additional file 4, Fig. S4).

A three-year follow-up of LABC patients was conducted to evaluate the curative effects of NCT and the rationality of the surrogate endpoints including Ki-67 changes. We set the media value of CTC numbers as a threshold, and divided subjects into a CTC-High and CTC-Low group. The comparison of progression-free survival (PFS) and overall survival (OS) between the two groups was performed using Log-rank test. Results show that patients with higher CTC numbers exhibited a significantly shorter PFS and OS compared to those in the CTC-Low group after the 8th NCT course (Fig. 6D and E). In addition, we evaluated the survival of patients with High-R and Low-R (according to the Ki-67 index) and found patients in the High-R group had significantly higher PFS and OS than patients in the Low-R group (Additional file 5, Fig. S5), which confirms the high reliability of the grouping methods.

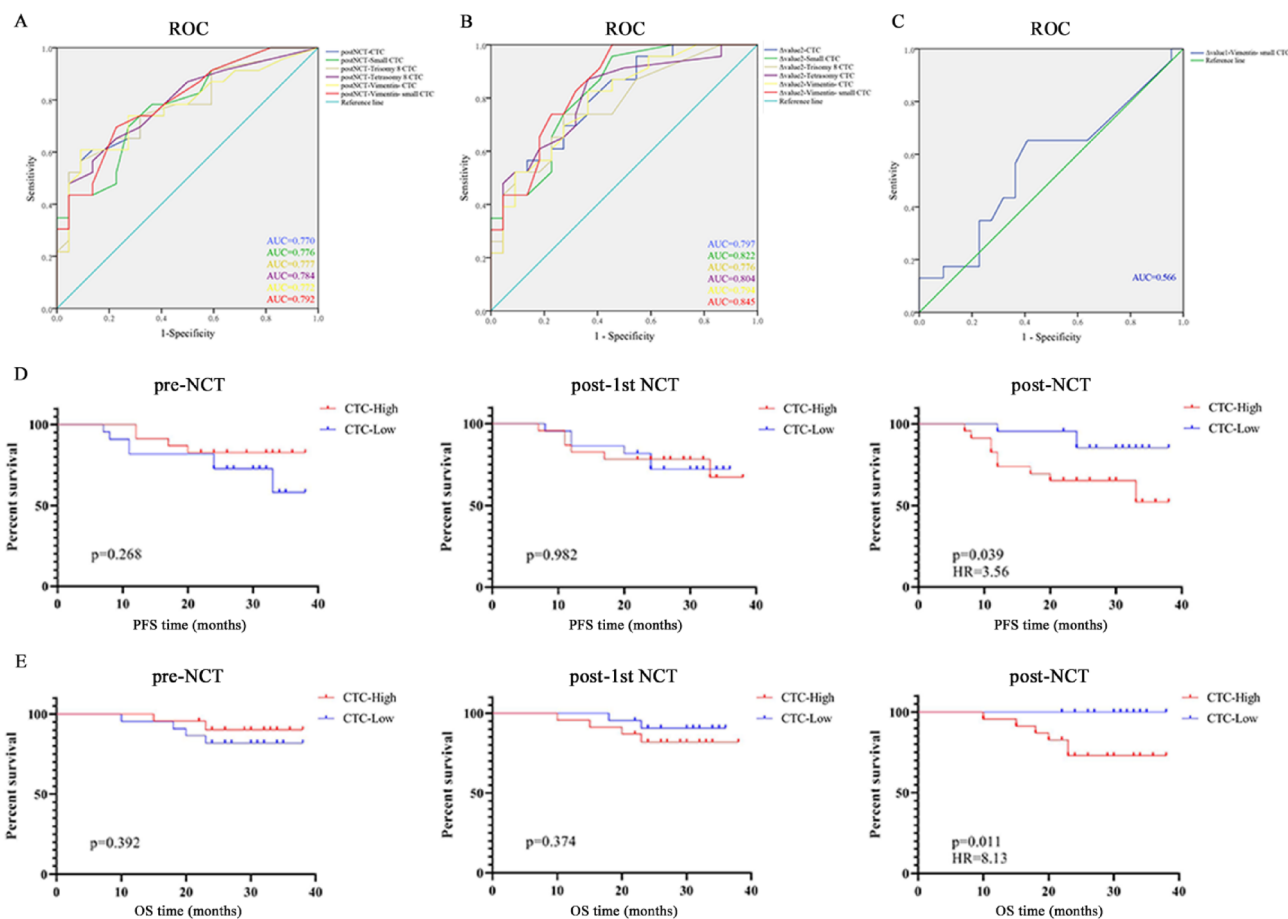


Fig. 6 Receiver operating characteristic (ROC) curves for CTC numbers with different heterogeneities for discriminating low response from high-response and prognostic value of the CTC numbers for LABC patients. AUC: area under the curve. **A** Number of CTCs and heterogeneities of CTC after the eighth course of NCT. **B** Δ value2

(difference between the third and the first timepoints) of CTCs and CTC heterogeneities. **C** The Δ value1 (difference between the second and the first timepoints) of vimentin⁻ + small-size CTCs. **D** Progression-free survival analysis for LABC patients receiving NCT. **E** Overall survival analysis for LABC patients receiving NCT

Discussion

Liquid biopsy is the focus of precision oncology as it is noninvasive and can be repeated at multiple time points, facilitating the monitoring of disease courses and therapy selection [21]. Recent study demonstrated that the prognostic effect of CTC status before and after therapy varies through time, and indicated CTC detection pre- and post-adjuvant chemotherapy can predict early relapse, supporting investigations for novel adjuvant therapeutic approaches [22]. However, the predictive value of CTCs for NCT response remains controversial. CTC detection clinical trials based on the CellSearch® system suggested EpCAM-positive CTC counts were not correlated to pCR in NCT [23, 24]. Our previous study demonstrated that systemic adjuvant chemotherapy had a significant impact on CTCs, as assessed via RT-PCR, and this effect was observed after three cycles of chemotherapy [7]. The data also indicated the decline of CTC-positive rates in NCT, which emboldened the rationale for use of CTCs as a biomarker in NCT response monitoring [25]. These inconsistent results may be due to the use of different detection platforms. Mego and colleagues measured CTC by CellSearch® or AdnaTest™ and their results demonstrated that epithelial-mesenchymal transition (EMT) phenotype CTCs may occur in the peripheral circulation of patients, and NCT is unable to eliminate CTCs undergoing EMT [26].

In the present study, the SE-i-FISH® platform was used for CTC detection and characterization. Recently, this method has been validated for detection of various rare tumor cells including CTCs [27–33]. Based on the existing evidence on the effectiveness of this method, the present study did not choose another method to repeat the verification of CTCs. SE-i-FISH® effectively isolates CTCs without hypotonic damage and detects different heterogeneous CTCs regardless of size variation and epithelial or mesenchymal phenotypes. In this study, the positive CTC rate is similar to the results presented by Camara and colleague [34], yet higher than those reported by other researchers [35, 36]. Several factors may account for this discrepancy. First, our results proved Fisher's theory that hematogenous metastasis could be found in early phase breast cancer, as it is a systematic disease [37, 38]. The patients enrolled in this study were diagnosed at the locally advanced stage, making the presence of CTCs extremely likely. Patients with more than two lymph node metastases did have more CTCs. Secondly, the SE-i-FISH® platform detected CTCs by various tumor markers and chromosome karyotype, which should improve the overall detection rate. The high sensitivity of this technique has been verified in other malignancies including cancers of the liver, lung, colorectum, and kidneys [27, 29].

One of the most remarkable results of our study was an observed obvious increase in CTC numbers (both total and heterogeneous) after the first course of NCT that was maintained at a high level until surgery. A similar elevation following the first course of NCT has been reported in a previous study, although different CTC capture rates existed due to the different testing methods; researchers found that CTC numbers increased concomitantly with taxane-induced tumor size-reduction [34]. More focus is placed on the changes between the baseline and post-NCT CTC numbers. A meta-analysis suggested that CTC counts decreased after NCT compared to the baseline [4]. However, this study used the CellSearch® System as the only detection method, and chemotherapy may have a substantial impact on epithelial and mesenchymal phenotypes. Hence, there were considerable differences between our SE-i-FISH® platform-based results and previous studies.

Changes in proliferation are a prerequisite for changes in tumor growth rate and a decrease in the Ki-67 proliferation index during NCT is predictive of long-term benefits [39, 40]. A large reduction in Ki-67 indicates that NCT may be effective. Alternatively, a small reduction, unchanged, or increased Ki-67 indicate that NCT may be ineffective. Some researchers have argued that although a tumor may exhibit a large initial decrease in the Ki-67 index, if it remains high after NCT there remains a high risk of recurrence [41]. Unlike the prognostic model in our earlier study, the chemotherapy response prediction model was applied in the present study. Ki-67 index fluctuation is the best group standard test to distinguish different tumor cell sensitivities to chemotherapy.

The Miller–Payne system was constructed in 2003, [17] and was generally accepted by oncologists. It was applied to patient groupings in this study to analyze the correlation between CTCs and clinical response. Herein, eight patients were classified as Miller–Payne grade 4 or 5 after NCT, all of whom had a high Ki-67 index reduction. By this standard, the trend in variation was the same as the Ki-67 grouping (data presented in supplementary material). However, due to the extremely uneven sample numbers (8 vs 37), further assessment is required with a larger survey sample.

The comparison of CTC numbers at different time points based on chemotherapy response grouping is of high clinical value. As treatment progresses, the difference between CTC levels in High-R and Low-R groups increased. The continuous rise of CTC numbers in the Low-R group was the most notable trend. The general upward trend of CTC numbers with time may be attributed to the increase in the Low-R group in this study. Tumor response to chemotherapy may be related to the increase of CTC after the first treatment. At later stages of NCT, apoptotic CTCs were eliminated, which would explain the CTC decrease in the final measurement. But in Low-R

patients, the increase in CTC number after NCT cannot be completely attributed to apoptotic cells. In Low-R patients, the primary tumors exhibited chemotherapy resistance. The corollary of this phenomenon is that CTCs possess proliferative capacity. The CTC elevation in this group may be unrelated to apoptosis, and active CTCs may be predominant. It is necessary to detect the proliferative capacity of CTC in future studies.

Spontaneous chromosome mis-segregation events in aneuploid cells promote chromosomal instability (CIN) that can give rise to intrinsic multidrug resistance compared to CIN- cell lines [42]. Several studies have demonstrated a correlation between Chr8 ploidy in CTCs and chemotherapy resistance in different tumors [28, 43–45]. In advanced gastric cancer, triploid Chr8 CTCs exhibited intrinsic drug resistance, whereas tetra- and multiploid CTCs may develop acquired resistance following chemotherapy [43]. The drug resistance character of triploid Chr8 CTCs was also observed in nasopharyngeal carcinoma [28] and locally advanced rectal cancer. To our knowledge, this study analyzed the quantity and proportion of Chr8 aneuploidy in NCT at different time points grouped by chemotherapy response for the first time in patients with LABC. During NCT, the number of triploid and tetraploid Chr8 CTCs increased only in the Low-R group. More importantly, an increasing proportion with time was found in the Low-R group.

Traditional methods marked by the CellSearch® System and RT-PCR are incapable of identifying CTC size. Complementary techniques such as ISET (isolation by size of epithelial tumor cells), based on a direct size selection method for epithelial cell enrichment to further filter small CTCs may be applied to generate additional information. Research has shown the number of small CTCs is increased following chemotherapy and is accompanied by the increased ratio of drug-resistant to drug-sensitive CTCs [46]. CTMs, derived from oligoclonal groups of cells from the primary tumor, have a 23- to 50-fold increased metastatic potential compared to single CTCs [47]. In the present study, both small-size CTCs and CTMs were detected; an increase in small CTCs over the course of chemotherapy was found. We attribute the overall increase of small CTC number to the increase seen in the Low-R patients. In contrast, no significant changes in CTM number occurred during NCT, indicating that CTM may have a closer relationship with metastasis than drug resistance. Although primary understanding of the small CTCs and CTM associated with drug resistance has been ascertained through SE-iFISH system in this study, the research on these two types of CTCs was still at an initial stage. It would be necessary to know if the small CTC are from apoptotic/necrotic/dying cells to be stained with cell death markers. But the number of fluorescent channels is limited. We can only arrange the limited fluorescence channels properly, and there is no redundancy. Questions like

cytoactive of CTCs was inevitably set to play an increasingly important role for researchers.

Some studies have indicated that CTCs with an EMT phenotype may occur in the peripheral circulation of patients with breast cancer [26]. Patients with vimentin⁺ CTCs had worse survival rates than those with CK⁺ CTCs [48]. In this study, results show the close relationship between vimentin⁻ CTC numbers (large and small CTCs) and low therapy response. The proportion of vimentin⁻ CTCs and small CTCs increased throughout the Low-R group. Notably, an increase then decrease of mesenchymal CTCs was found during NCT, especially in large CTCs of the High-R group. There is no clear explanation for this phenomenon to date. Chemotherapy could promote the EMT of primary tumor cells by multiple pathways [49] resulting in the initial increase. A study has provided evidence that EMT tumor cells modulate NK cell ligands and are vulnerable to NK-mediated cytotoxicity [50]; activation of the innate immune system may result in decreasing numbers over time.

Positive correlations between CTCs and blood cells (neutrophils and platelets) were also observed before NCT. During the metastatic process, cancer cells encounter many other circulating cells. Several studies have shown that circulating platelets and neutrophils contribute to the binding of cancer cells to the endothelium and to their extravasation across the endothelial barrier [51–53]. However, throughout the course of NCT, this correlation disappeared due to the myelosuppression caused by chemotherapy.

The diagnostic efficacy of CTCs in distinguishing different chemotherapeutic responses was tested in this study. Effective performance correlations were demonstrated for almost all indicators described based upon determinations made before surgery. However, if predicting the NCT response based only on the CTC number post-first course, the only relatively accurate indicator was the Δ value1 of vimentin- small-size CTCs. The well-known SWOG S0500 clinical trial demonstrated that for patients with persistently increased CTCs after 21 days of first-line chemotherapy, early switching to an alternative cytotoxic therapy was ineffective in prolonging overall survival [54]. Our study also found low diagnostic performance after one course of chemotherapy. However, it is expected that testing over a longer timeframe will result in higher forecasting performance with this new CTC detection platform.

Although surrogate endpoints including the Ki-67 and Miller–Payne system are commonly accepted, it is widely accepted that these methods carry with them a certain level of inherent risk. Therefore, in the present study, our follow-up outcome was used to evaluate the grouping methods and to overcome the skepticism. Kim and colleagues reported elimination of CTCs could prevent metastasis and extend survival [55]. In our study, patients with High-R showed lower recurrence than those in the Low-R. More importantly, we

observed specific significant differences between PFS and OS and patients with different levels of CTCs. Cumulatively, these results confirm that CTC numbers could be used as an evaluation index for the prognosis of LABC.

As an observational study, we basically achieved our research objectives. Randomized controlled studies with larger sample sizes will help change clinical decision making in the future.

Conclusions

During a typical NCT course-specific CTCs in peripheral blood may allow for rapid evaluation of NCT response. Detection at additional time points may increase the predictive capacity of CTCs to improve unfavorable outcome rates in LABC patients.

Supplementary Information The online version contains supplementary material available at <https://doi.org/10.1007/s10549-023-06942-y>.

Acknowledgements The authors wish to thank all the patients and family members for participating in this study.

Author contributions GM carried out the conceptualization, project administration, formal analysis, writing – original draft, and writing – review and editing. JW carried out project administration and data analysis. JF carried out the data curation and methodology. RC participated in project administration and data processing. ML participated in writing – original draft and writing – review and editing. ML carried out the data analysis. TX carried out the conceptualization and project administration. XL carried out the conceptualization and funding acquisition. SW carried out the conceptualization, supervision, and funding acquisition.

Funding This work was supported by the Natural Science Foundation of China (81572607, 82203118 and 81572602).

Data availability All data generated or analyzed during this study are included in this published article and its supplementary information files. Other remaining data and materials are available from the authors upon reasonable request.

Declarations

Conflict of interest The authors declared no potential conflicts of interest. Prior presentation: This work has been presented in part at the 2019 ASCO Annual Meeting.

Ethical approval Samples were collected at the First Affiliated Hospital with Nanjing Medical University. Ethics approval was obtained from the institutional ethics committee of the First Affiliated Hospital with Nanjing Medical University.

Informed consent Written informed consent was obtained from all participants.

References

- Sung H et al (2021) Global cancer statistics 2020: GLOBOCAN estimates of incidence and mortality worldwide for 36 cancers in 185 countries. *CA Cancer J Clin* 71(3):209–249
- Yamauchi K et al (2008) Induction of cancer metastasis by cyclophosphamide pretreatment of host mice: an opposite effect of chemotherapy. *Cancer Res* 68(2):516–520
- Comen E, Norton L, Massagué J (2011) Clinical implications of cancer self-seeding. *Nat Rev Clin Oncol* 8(6):369–377
- Bidard FC et al (2018) Circulating tumor cells in breast cancer patients treated by neoadjuvant chemotherapy: a meta-analysis. *J Natl Cancer Inst* 110(6):560–567
- Caixeiro NJ et al (2014) Circulating tumour cells—a bona fide cause of metastatic cancer. *Cancer Metastasis Rev* 33(2–3):747–756
- Molloy TJ et al (2011) The prognostic significance of tumour cell detection in the peripheral blood versus the bone marrow in 733 early-stage breast cancer patients. *Breast Cancer Res* 13(3):R61
- Chong MH et al (2012) The dynamic change of circulating tumour cells in patients with operable breast cancer before and after chemotherapy based on a multimarker QPCR platform. *Br J Cancer* 106(10):1605–1610
- van Dalum G et al (2015) Circulating tumor cells before and during follow-up after breast cancer surgery. *Int J Oncol* 46(1):407–413
- Nolé F et al (2008) Variation of circulating tumor cell levels during treatment of metastatic breast cancer: prognostic and therapeutic implications. *Ann Oncol* 19(5):891–897
- Pierga JY et al (2017) Circulating tumour cells and pathological complete response: independent prognostic factors in inflammatory breast cancer in a pooled analysis of two multicentre phase II trials (BEVERLY-1 and -2) of neoadjuvant chemotherapy combined with bevacizumab. *Ann Oncol* 28(1):103–109
- Riethdorf S et al (2017) Prognostic impact of circulating tumor cells for breast cancer patients treated in the neoadjuvant “Geparquattro” trial. *Clin Cancer Res* 23(18):5384–5393
- Andergassen U et al (2016) Real-time RT-PCR systems for CTC detection from blood samples of breast cancer and gynaecological tumour patients (review). *Oncol Rep* 35(4):1905–1915
- Ozkumur E et al (2013) Inertial focusing for tumor antigen-dependent and -independent sorting of rare circulating tumor cells. *Sci Transl Med* 5(179):17947
- Passerini V et al (2016) The presence of extra chromosomes leads to genomic instability. *Nat Commun* 7:10754
- Gordon DJ, Resio B, Pellman D (2012) Causes and consequences of aneuploidy in cancer. *Nat Rev Genet* 13(3):189–203
- Kops GJ, Weaver BA, Cleveland DW (2005) On the road to cancer: aneuploidy and the mitotic checkpoint. *Nat Rev Cancer* 5(10):773–785
- Ogston KN et al (2003) A new histological grading system to assess response of breast cancers to primary chemotherapy: prognostic significance and survival. *Breast* 12(5):320–327
- Lin PP (2015) Integrated EpCAM-independent subtraction enrichment and iFISH strategies to detect and classify disseminated and circulating tumors cells. *Clin Transl Med* 4(1):38
- Lin PP et al (2017) Comprehensive in situ co-detection of aneuploid circulating endothelial and tumor cells. *Sci Rep* 7(1):9789
- Magee R, Rigoutsos I (2020) On the expanding roles of tRNA fragments in modulating cell behavior. *Nucleic Acids Res* 48(17):9433–9448
- Heitzer E et al (2019) Current and future perspectives of liquid biopsies in genomics-driven oncology. *Nat Rev Genet* 20(2):71–88

22. Matikas A et al (2022) Detection of circulating tumour cells before and following adjuvant chemotherapy and long-term prognosis of early breast cancer. *Br J Cancer* 126(11):1563–1569
23. Pierga JY et al (2008) Circulating tumor cell detection predicts early metastatic relapse after neoadjuvant chemotherapy in large operable and locally advanced breast cancer in a phase II randomized trial. *Clin Cancer Res* 14(21):7004–7010
24. Onstenk W et al (2015) Improved circulating tumor cell detection by a combined EpCAM and MCAM cell search enrichment approach in patients with breast cancer undergoing neoadjuvant chemotherapy. *Mol Cancer Ther* 14(3):821–827
25. Kasimir-Bauer S et al (2016) Does primary neoadjuvant systemic therapy eradicate minimal residual disease? Analysis of disseminated and circulating tumor cells before and after therapy. *Breast Cancer Res* 18(1):20
26. Mego M et al (2012) Expression of epithelial-mesenchymal transition-inducing transcription factors in primary breast cancer: The effect of neoadjuvant therapy. *Int J Cancer* 130(4):808–816
27. Li X et al (2018) Clinical significance of detecting CSF-derived tumor cells in breast cancer patients with leptomeningeal metastasis. *Oncotarget* 9(2):2705–2714
28. Zhang J et al (2018) Circulating tumor cells with karyotyping as a novel biomarker for diagnosis and treatment of nasopharyngeal carcinoma. *BMC Cancer* 18(1):1133
29. Ye Z et al (2019) Detecting and phenotyping of aneuploid circulating tumor cells in patients with various malignancies. *Cancer Biol Ther* 20(4):546–551
30. Luo S et al (2021) Optimal strategy for colorectal cancer patients' diagnosis based on circulating tumor cells and circulating tumor endothelial cells by subtraction enrichment and immunostaining-fluorescence in situ hybridization combining with CEA and CA19-9. *J Oncol* 2021:1517488
31. Lin AY et al (2021) Identification and comprehensive co-detection of necrotic and viable aneuploid cancer cells in peripheral blood. *Cancers (Basel)* 13(20):5108
32. Zhang T et al (2021) Role of aneuploid circulating tumor cells and CD31(+) circulating tumor endothelial cells in predicting and monitoring anti-angiogenic therapy efficacy in advanced NSCLC. *Mol Oncol* 15(11):2891–2909
33. Mi J et al (2022) Case report: post-therapeutic laryngeal carcinoma patient possessing a high ratio of aneuploid CTCs to CTCs rapidly developed de novo malignancy in pancreas. *Front Oncol* 12:981907
34. Camara O et al (2007) The relevance of circulating epithelial tumor cells (CETC) for therapy monitoring during neoadjuvant (primary systemic) chemotherapy in breast cancer. *Ann Oncol* 18(9):1484–1492
35. Ignatiadis M et al (2008) Prognostic value of the molecular detection of circulating tumor cells using a multimarker reverse transcription-PCR assay for cytokeratin 19, mammaglobin A, and HER2 in early breast cancer. *Clin Cancer Res* 14(9):2593–2600
36. Pachmann K et al (2008) Monitoring the response of circulating epithelial tumor cells to adjuvant chemotherapy in breast cancer allows detection of patients at risk of early relapse. *J Clin Oncol* 26(8):1208–1215
37. Fisher B, Fisher ER (1967) The organ distribution of disseminated 51 Cr-labeled tumor cells. *Cancer Res* 27(2):412–420
38. Fisher B, Fisher ER, Feduska N (1967) Trauma and the localization of tumor cells. *Cancer* 20(1):23–30
39. Miglietta L et al (2010) Prognostic value of estrogen receptor and Ki-67 index after neoadjuvant chemotherapy in locally advanced breast cancer expressing high levels of proliferation at diagnosis. *Oncology* 79(3–4):255–261
40. Li L et al (2017) Prognostic values of Ki-67 in neoadjuvant setting for breast cancer: a systematic review and meta-analysis. *Future Oncol* 13(11):1021–1034
41. Miglietta L et al (2013) A prognostic model based on combining estrogen receptor expression and Ki-67 value after neoadjuvant chemotherapy predicts clinical outcome in locally advanced breast cancer: extension and analysis of a previously reported cohort of patients. *Eur J Surg Oncol* 39(10):1046–1052
42. Lee AJ et al (2011) Chromosomal instability confers intrinsic multidrug resistance. *Cancer Res* 71(5):1858–1870
43. Li Y et al (2014) Clinical significance of phenotyping and karyotyping of circulating tumor cells in patients with advanced gastric cancer. *Oncotarget* 5(16):6594–6602
44. Wan JF et al (2018) Aneuploidy of chromosome 8 and mutation of circulating tumor cells predict pathologic complete response in the treatment of locally advanced rectal cancer. *Oncol Lett* 16(2):1863–1868
45. Li Y et al (2018) Evolutionary expression of HER2 conferred by chromosome aneuploidy on circulating gastric cancer cells contributes to developing targeted and chemotherapeutic resistance. *Clin Cancer Res* 24(21):5261–5271
46. Ito H et al (2016) Change in number and size of circulating tumor cells with high telomerase activity during treatment of patients with gastric cancer. *Oncol Lett* 12(6):4720–4726
47. Aceto N et al (2014) Circulating tumor cell clusters are oligoclonal precursors of breast cancer metastasis. *Cell* 158(5):1110–1122
48. Zhang D et al (2017) Circulating tumor microemboli (CTM) and vimentin+ circulating tumor cells (CTCs) detected by a size-based platform predict worse prognosis in advanced colorectal cancer patients during chemotherapy. *Cancer Cell Int* 17:6
49. Li QQ et al (2011) Involvement of NF-kappaB/miR-448 regulatory feedback loop in chemotherapy-induced epithelial-mesenchymal transition of breast cancer cells. *Cell Death Differ* 18(1):16–25
50. Chockley PJ et al (2018) Epithelial-mesenchymal transition leads to NK cell-mediated metastasis-specific immunosurveillance in lung cancer. *J Clin Invest* 128(4):1384–1396
51. Somasundaram R, Herlyn D (2009) Chemokines and the micro-environment in neuroectodermal tumor-host interaction. *Semin Cancer Biol* 19(2):92–96
52. Coupland LA, Chong BH, Parish CR (2012) Platelets and P-selectin control tumor cell metastasis in an organ-specific manner and independently of NK cells. *Cancer Res* 72(18):4662–4671
53. Reymond N, d'Agua BB, Ridley AJ (2013) Crossing the endothelial barrier during metastasis. *Nat Rev Cancer* 13(12):858–870
54. Smerage JB et al (2014) Circulating tumor cells and response to chemotherapy in metastatic breast cancer: SWOG S0500. *J Clin Oncol* 32(31):3483–3489
55. Kim YR et al (2018) Selective killing of circulating tumor cells prevents metastasis and extends survival. *J Hematol Oncol* 11(1):114

Publisher's Note Springer Nature remains neutral with regard to jurisdictional claims in published maps and institutional affiliations.

Springer Nature or its licensor (e.g. a society or other partner) holds exclusive rights to this article under a publishing agreement with the author(s) or other rightsholder(s); author self-archiving of the accepted manuscript version of this article is solely governed by the terms of such publishing agreement and applicable law.